nature neuroscience

Cortical reorganization consistent with spike timing–but not correlation-dependent plasticity

Joshua M Young[1–3], Wioletta J Waleszczyk[3,4], Chun Wang[3], Michael B Calford[5], Bogdan Dreher[3] & Klaus Obermayer[1,2]

The receptive fields of neurons in primary visual cortex that are inactivated by retinal damage are known to 'shift' to nondamaged retinal locations, seemingly due to the plasticity of intracortical connections. We have observed in cats that these shifts occur in a pattern that is highly convergent, even among receptive fields that are separated by large distances before inactivation. Here we show, using a computational model of primary visual cortex, that the observed convergent shifts are inconsistent with the common assumption that the underlying intracortical connection plasticity is dependent on the temporal correlation of pre- and postsynaptic action potentials. The shifts are, however, consistent with the hypothesis that this plasticity is dependent on the temporal order of pre- and postsynaptic action potentials. This convergent reorganization seems to require increased neuronal gain, revealing a mechanism that networks may use to selectively facilitate the didactic transfer of neuronal response properties.

Neuronal activity seems to play a crucial role in the organization of synaptic connectivity during development[1,2]. Two 'Hebbian'[3] hypotheses have emerged that attempt to describe how the long-term efficacy of a synapse is modulated by pre- and postsynaptic activity. The first hypothesis, which we call correlation-dependent plasticity (CDP), states that when a pre- and a postsynaptic neuron generate action potentials ('spikes') at a similar time, the synapses that connect them strengthen, regardless of the temporal order in which the spikes occurred[4,5]. The second hypothesis, referred to as spike timing–dependent plasticity (STDP), claims that the temporal order of the spikes determines whether the synapses are potentiated or depressed[6–11]. Viewpoints among both experimentalists and theoreticians conflict on which of these rules is more important for determining the response properties of a neuron, in particular the organization of its receptive field[12–22].

It is recognized that the effects of STDP should be apparent not only in the changes to the receptive fields of single neurons, but also in the pattern of these changes among multiple neurons[18]. It has been predicted that, within a population of neurons with STDP at their interconnections, any neuron that frequently initiates activity among its neighbors will influence them to develop response properties that resemble its own[18]. As previously described[18], this property of STDP can be understood by considering the example of two reciprocally connected neurons 'A' and 'B': if neuron A spikes before neuron B, STDP will potentiate the input connection of neuron A to neuron B; however, the input connection of neuron B to neuron A will be depressed. The potentiation of the input from neuron A to neuron B will contribute to making the response properties of neuron B more similar to those of neuron A. In addition, any other input connections to neuron B that were active before its spike will also be potentiated, and these may include shared input connections that contributed to spike initiation in neuron A. Thus, neuron B will further increase the similarity of its response properties to those of neuron A by imitating the pattern of connectivity of neuron A. Because any increase in the similarity of the response properties of neurons A and B is achieved through changes to the input connections of neuron B, this activity-dependent reorganization can be described as 'didactic'.

In contrast to the situation under STDP, under CDP the activity sequence described above would cause the A to B and B to A connections to undergo an identical modification, making any increase in the similarity of their response properties the result of changes in the input connectivity of both neurons. Thus, didactic reorganization, in which a 'teacher' neuron transfers its response properties to a 'student' neuron[18], can occur as a consequence of STDP but not CDP. Evidence showing that the response properties of neurons *in vivo* have undergone didactic reorganization would, therefore, be a strong indication that their input connections are subject to STDP.

According to the hypothesis described above, didactic reorganization generated by STDP should be more apparent among neurons that have low stimulus selectivity, because such neurons are more likely to respond to the same stimulus events and thus have spike timing differences short enough to fall within the STDP window observed *in vivo*[7,9,10,18]. Therefore, the likelihood of observing didactic reorganization should be greater during development or after some form of

[1]Neural Information Processing Group, Department of Electrical Engineering and Computer Science, Berlin University of Technology, FR 2-1, Franklinstrasse 28/29, D-10587 Berlin, Germany. [2]Bernstein Center for Computational Neuroscience, Humboldt University Berlin, Philippstrasse 13, House 6, 10115 Berlin, Germany. [3]Bosch Institute, Anderson Stuart Building (F13), Eastern Avenue, University of Sydney, 2006 New South Wales, Australia. [4]Nencki Institute of Experimental Biology, Pasteur 3, 02-093 Warsaw, Poland. [5]School of Biomedical Sciences and Hunter Medical Research Institute, Callaghan Campus, The University of Newcastle, Newcastle, 2308 New South Wales, Australia. Correspondence should be addressed to J.M.Y. (joshua.young@bccn-berlin.de) or K.O. (oby@cs.tu-berlin.de).

Received 9 February; accepted 30 April; published online 27 May 2007; doi:10.1038/nn1913

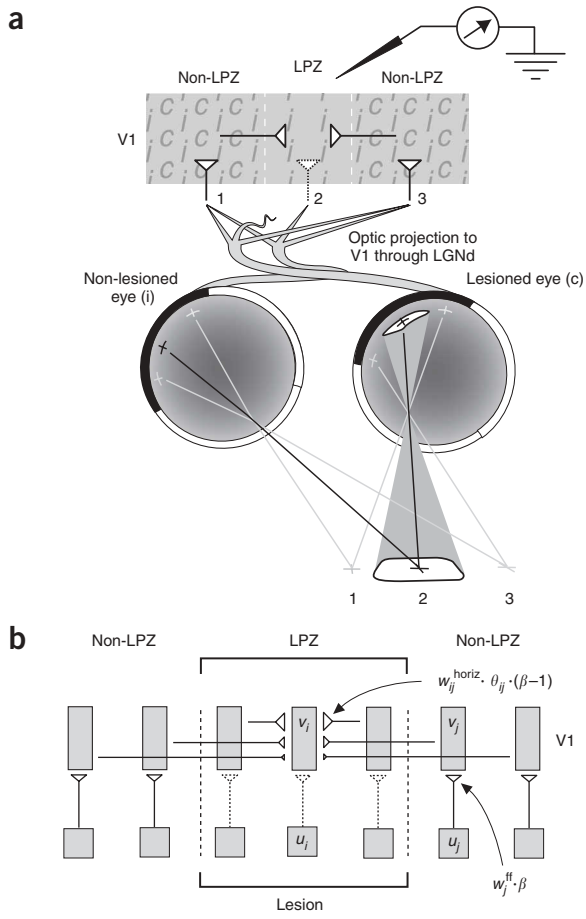

Figure 1 Measurement and modeling of retinal lesion–induced receptive field reorganization in V1. (**a**) Topographic projection of visual input from the lesioned (contralateral, c) and nonlesioned (ipsilateral, i) eyes to V1. Three points in visual space (shaded crosses) project to three pairs of corresponding points in the retinas. The ordered projection of feedforward input connections to V1 (represented as vertical lines and triangular synapses) ensure that each binocular neuron integrates input from the two eyes corresponding to roughly the same point in visual space (point 1, 2 or 3). Owing to the monocular retinal lesion, a circumscribed region of cortex ('lesion projection zone' or 'LPZ') has lost its feedforward input from the contralateral eye, but remains responsive to stimuli presented to this eye through input provided via long-range horizontal connections[33–35,44] (represented as horizontal lines and triangular synapses). LGNd, dorsal lateral geniculate nucleus. (**b**) The model network. Outside its lesioned region, a subcortical layer (squares, bottom row) provided feedforward input to a network of cortical columns (rectangles, top row) through connections of strength w_i^{ff}. The firing probability among excitatory neurons in each subcortical or cortical population was u_i and v_i, respectively. Input was exchanged between the columns through horizontal connections of strength w_{ij}^{horiz}. All column inputs had both excitatory and inhibitory effects, and their balance was determined by β. The responsiveness of a column to horizontal input was also affected by transient suppression arising from previous inputs, a phenomenon represented by θ_{ij} (see equation (2), Methods).

input loss, because both situations are associated with transient stages of low stimulus selectivity[23,24] and enhanced plasticity[25–28].

With this reasoning, we have investigated whether didactic reorganization can be observed *in vivo* through a combination of both of these 'low-selectivity' scenarios. In adolescent cats, we eliminated the feedforward input (from the contralateral eye) to a small region in the binocular segment of primary visual cortex (area V1, striate cortex, cytoarchitectonic area 17) through the creation of a circumscribed monocular retinal lesion (**Fig. 1a**). We subsequently measured the resulting receptive field location changes of V1 neurons in this partially deprived zone, and developed a model of lesion-induced receptive field reorganization for comparison (**Fig. 1b**). In the simulated reorganization, deprived cortical neurons had their response selectivity lowered by a uniform increase in the efficacy of all of their excitatory input connections (described as an increase in 'neuronal gain'). The efficacies of the intracortical input connections to these neurons were then subjected to activity-based modification through either CDP or STDP. We observed that, although the *in vivo* receptive fields were often shifted in a parallel or convergent pattern, the simulated receptive field shifts produced by CDP diverged radially outwards from the lesion center. When the model combined STDP and high neuronal gain, however, the convergence observed among the *in vivo* receptive field shifts was robustly reproduced. In addition, using the estimated shapes of the deprived cortical zones *in vivo* to designate the deprived region in the model biased the reorganization toward producing the same directions of receptive field convergence as observed in our experiments. Further analysis leads us to conclude that the receptive field convergence observed *in vivo* arises from a didactic reorganization of intracortical connectivity via STDP. We also conclude that this convergence takes place when the spatial range over which didactic reorganization can occur is extended by a homeostatic increases in neuronal gain.

RESULTS

Receptive field reorganization *in vivo*

We created circumscribed monocular retinal lesions in five cats during the peak of the postnatal critical period for plasticity in V1 (ref. 25; **Fig. 1a** and Methods). Between 7 and 16 months later, we made extracellular recordings in each cat from V1 neurons in the deprived zone created by the retinal lesion ('lesion projection zone'). A quantitative description of the ocular dominance, receptive field size, orientation tuning and velocity response properties, and some examples of the receptive field locations of these neurons have been previously reported, as part of a comparison of the recovery of V1 responses after retinal lesions made in either adulthood or adolescence[28]. To ensure that we had defined the area of retinal damage correctly, we made a postmortem count of the α retinal ganglion cells in each lesioned retina (**Fig. 2**). In one cat (KR1), there seemed to be retrograde degeneration, peripheral to the lesion, along the estimated retinal ganglion cell axon paths[28,29]. This degeneration was taken into account in our subsequent modeling work (**Supplementary Methods** online).

In nonlesioned cats, the ipsilateral and contralateral eye receptive fields of binocular neurons correspond, within a few degrees, to the same position in visual space (**Fig. 2**). Consistent with the results of previous studies[27,30,31], we observed a smooth progression of receptive field locations in the nonlesioned eye as the recording electrode moved from outside to inside the lesion projection zone (**Supplementary Figs. 1** and **2** and **Supplementary Results** online). Because this smooth progression indicated that the nonlesioned eye receptive fields did not change location as a result of the lesion, we used the location of each binocular neuron's receptive field in the nonlesioned eye as an estimate of the pre-lesion location of its receptive field in the lesioned eye[27,30,31]. Consistent with previous reports[26,27,30–34], this approach revealed that the lesioned-eye receptive fields of these binocular neurons had undergone extensive positional shifts (**Fig. 2**). A new experimental observation, however, was that the lesioned-eye receptive fields rarely shifted toward the closest region of available intact retina but instead

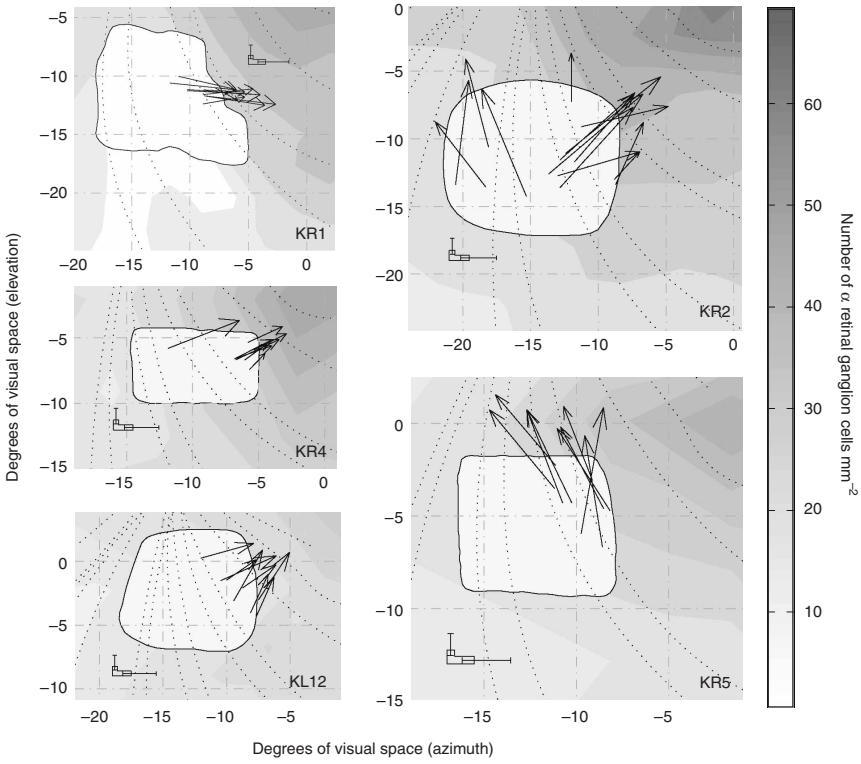

Figure 2 Shifts in receptive field location among neurons in the cortical lesion projection zone of five cats (KR1, KR2, KR4, KR5, KL12). Each panel shows the lesioned area (white), the estimated paths of retinal ganglion axons[29] (curved dotted lines) and the measured densities of α retinal ganglion cells (unbroken contours) of the lesioned retina. All of these features are represented in visual space (tangent projection, degrees of azimuth and elevation relative to the area centralis), but each panel is scaled independently to improve clarity. Each arrow denotes the shift in the lesioned-eye receptive field of a binocular neuron in the lesion projection zone in V1: the base and tip of the arrow mark the center of, respectively, the nonlesioned-eye and lesioned-eye receptive fields of the neuron. The median and the first and third quartiles of the absolute horizontal and vertical differences in the positions of the ipsilateral- and the contralateral-eye receptive fields of binocular neurons ($n = 74$) recorded in nonlesioned cats are indicated in each panel by the L-shaped bar and its error markers. In each cat except KR1, the α retinal ganglion cell distribution seems to have a normal density gradient running from the area centralis to the periphery. In KR1, degeneration can be seen below the lesion, corresponding to the estimated paths of retinal ganglion axons that pass through the lesion.

converged to a common location (specific to each cat), even when separated by large distances before lesioning (**Fig. 2**).

Receptive field reorganization in a network model of V1

Much evidence from previous retinal lesion experiments indicates that long-term changes in receptive field location are established through reorganization of the long-range horizontal connections intrinsic to V1 (refs. 33,34), and not by changes to feedforward[32] or inter-areal connections[35]. To investigate whether plasticity at horizontal connections could be expected to produce the receptive field shifts that we observed, we created a two-dimensional network model of post-lesion reorganization in V1.

The model comprised a 'cortical' layer of horizontally interconnected neuron populations (or 'columns') and a 'subcortical' feedforward input layer (**Fig. 1b** and Methods). The shape of each *in vivo* lesion projection zone in V1 was estimated by projecting the outline of the retinal lesion onto the topographic map of visual space in V1 (ref. 36). To facilitate comparison with the model results, we also projected the receptive field shifts observed *in vivo* onto this map. Next, in separate simulations, each lesion projection zone shape was centered on the model network and all columns inside the boundaries of a zone had their feedforward input abolished. The model included a homeostatic compensation for the decrease in activity among these input-deprived columns in which their internal balance of excitation and inhibition was altered, thereby increasing their responsiveness to external input (implemented by the β parameter; **Fig. 1b** and Methods). After the initial lesion-induced inactivity, this increase in 'neuronal gain' allowed columns in the lesion projection zone to respond to horizontal input from columns outside the zone. As a result, the receptive fields of columns inside the zone expanded into the area outside the retinal lesion, which also produced a concomitant shift in the apparent center of each receptive field.

To elicit a Hebbian reorganization of the horizontal connections inside the lesion projection zone, model columns outside the zone were driven by random feedforward input from the subcortical layer and in turn provided input to columns inside the zone through horizontal connections. The resulting patterns of activity were then used to alter the efficacy of the horizontal input connections of the lesion projection zone columns via either CDP or STDP (Methods). Long periods of reorganization via CDP or STDP caused columns inside the lesion projection zone to contract their suprathreshold receptive fields on the intact retina bordering the lesion.

In vivo and simulated reorganization: CDP

Previous modeling studies of cortical reorganization via CDP have assumed that neurons in a lesion projection zone will have low mean firing rates during reorganization owing to the absence of feedforward input[12,15,16]. Among the simulations described above, we investigated this assumption by using CDP in conjunction with small increases in neuronal gain after lesioning (raising β from 1 to $1 < \beta < 1.1$). The increase in gain caused receptive fields to expand and shift outward, but the average level of activity among columns inside the lesion projection zone remained lower than that of columns outside the zone. Combined with this distribution of activity, CDP caused columns in the lesion projection zone to gradually potentiate the mono- or polysynaptic connections that they received from the columns outside the zone that were closest to them (**Fig. 3**). This potentiation caused their receptive fields to contract but also to remain in the divergent shift pattern (projecting out from the core of the lesion or lesion projection zone), which was an immediate consequence of the initial increase in neuronal gain (**Fig. 3a**). The directions of these simulated receptive field shifts were, however, highly dissimilar to those of the shifts observed *in vivo*, which often converged toward a common location (in both the visual field and its V1 representation), despite their diverse locations before lesioning (**Fig. 3a**). Quantitative measurements of the 'vergence' of each receptive

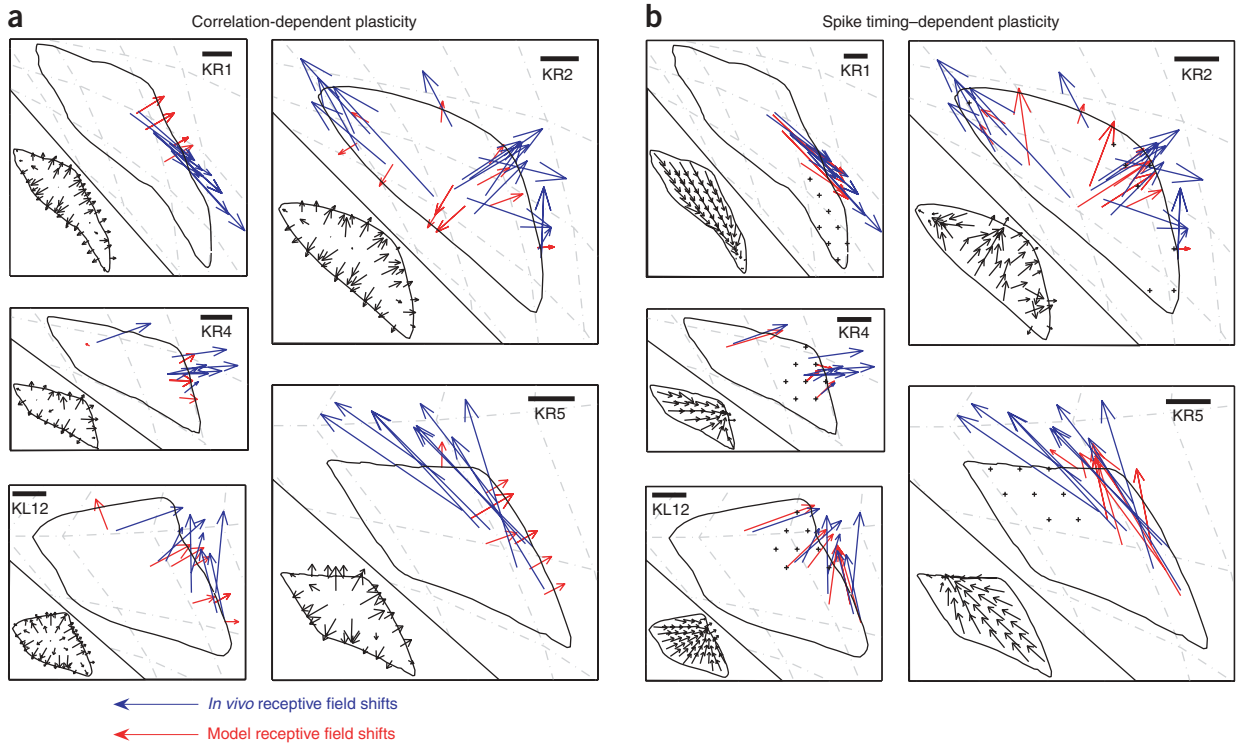

Figure 3 *In vivo* and simulated shifts of receptive field projected onto the representation of visual space in V1 (ref. 36). (**a**,**b**) Each panel illustrates the topographic map of visual space in V1, in which the curved broken lines correspond to the straight azimuth and elevation lines shown in **Figure 2**. Superimposed over this map is the estimated V1 lesion projection zone (black outline), and the corresponding shifts of the *in vivo* receptive fields (blue arrows). Also shown are the shifts of the simulated receptive fields (red arrows) produced by the model when either CDP (**a**) or STDP (**b**) was used. All of the model columns in the lesion projection zone showed a shift in their receptive field locations, but only those that had pre-lesion locations closest to the nonlesioned eye receptive fields of *in vivo* neurons are illustrated. Arrows in the lower left insets represent the change in the efficacies of the horizontal input connections of individual columns. For each column, the tip of the arrow is calculated as a weighted (by connection strength) mean of the locations of the columns that send input connections to that column. Thus, any column that has an arrow length greater than zero has developed a directional bias in the efficacy of its horizontal input connections. The '+' symbols in **b** indicate the model columns that maintained the shortest latencies of peak response during reorganization (see **Fig. 6**). Columns shown with receptive field shift arrows terminating in the lesion projection zone have split receptive fields. Scale bar, 1 mm.

field shift pattern (divergent versus convergent) confirmed this apparent difference between the *in vivo* and CDP simulation results (**Fig. 4a**,**b**).

We experimented with various modifications to the model and its parameters to find conditions under which CDP at horizontal connections could produce convergent receptive field shifts. This search included the combination of CDP with large increases in neuronal gain ($\beta > 1.1$), but the results were not congruous with known features of retinal lesion–induced reorganization *in vivo* (**Supplementary Results**). We also investigated the possibility that the *in vivo* receptive field convergence is a consequence of the potentiation of long-range horizontal connections between neurons with collinearly aligned receptive fields of similar orientation preference (**Supplementary Results**). A comparison between the orientation preference of each *in vivo* neuron and its receptive field shift direction strongly suggests, however, that this is not the case (**Supplementary Fig. 3**).

In vivo and simulated reorganization: STDP

We then investigated, using the same model, what kinds of receptive field shifts were produced when the efficacies of horizontal connections were governed by STDP[10]. When the post-lesion increase in neuronal gain was low ($1 < \beta < 1.1$), the receptive field shifts produced by STDP were largely indistinguishable from those produced by CDP. When larger gain increases were used ($\beta > 1.1$), however, STDP caused the model to reproduce the convergent character of the *in vivo* receptive field shifts (**Figs. 3b** and **4b**). This convergence is the consequence of a reorganization of the horizontal input connections inside the lesion projection zone that is qualitatively different to that produced by CDP. The direction in which the input connections to each column were potentiated was similar throughout the zone and was correlated with the direction of receptive field convergence (**Fig. 3b** and **Supplementary Videos** online). The direction of these connection changes and the convergence were found to be strongly dependent on the shape of the lesion projection zone: each estimated *in vivo* shape was conducive toward producing a convergence direction similar to that of the *in vivo* receptive field shifts associated with it (**Fig. 3b**). The convergence direction was also sensitive to the gain level inside the lesion projection zone during reorganization. The results shown in **Figures 3b** and **4b** were obtained by finding, separately for each shape of lesion projection zone, the gain level that produced the best match between the model and *in vivo* results (see also **Supplementary Fig. 4**). Notably, the optimized values of the neuronal gain for the different shapes were very similar ($\beta = 1.435$, KR1; 1.435, KR4; 1.45, KR5; 1.485, KL12), except for that associated with the KR2 shape ($\beta = 1.25$). For reasons explained in the next section, the lower gain value used for the KR2 simulation was needed to produce more than one receptive field convergence direction, as seems to have occurred *in vivo*.

In addition to the post-lesion increase in gain, two features of the model were important for producing the close match between the

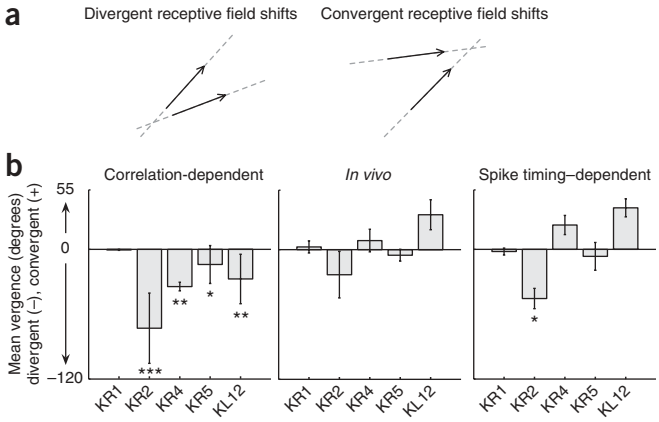

Figure 4 Convergence and divergence among the shifts of *in vivo* and simulated receptive fields. (**a**) The absolute angular difference between two receptive shifts (when represented in the V1 map of visual space) was multiplied by −1 or +1 depending on whether their lines of intersection were divergent or convergent. This measure was calculated for every paired combination of shifts recorded in a single cat, and a mean value for each shift across all of its pairings was calculated to create a distribution of 'vergence' values for each cat. (**b**) Means and standard deviations of the vergence distributions (see above) observed *in vivo* (middle) and produced by the model (**Fig. 3**) when it used either CDP (left) or STDP (right). The statistical significance of the difference between the vergence value distributions of the simulated and *in vivo* receptive field shifts are indicated: $^{*}P < 0.05$, $^{**}P < 0.01$, $^{***}P < 0.005$ (two-sided sign test, $n = 11$, KR1; $n = 15$, KR2; $n = 8$, KR4; $n = 9$, KR5; $n = 8$, KL12).

receptive field shifts that the model generated under STDP and those observed *in vivo* (**Figs. 3b** and **4b**). The first of these features was that, in the cortical layer of the model, activity propagated horizontally as waves[37,38] (implemented through the θ_{ij} function; Methods and **Fig. 1b**), thereby avoiding the generation of reverberatory feedback. Without this feature, the range of gain values that could produce receptive field convergence was significantly reduced. The second important feature was that, the horizontal distance between two columns affected the rate at which the connection between them could undergo changes in efficacy (implemented through the α_{ij} function; Methods). This feature did not influence whether or not receptive field convergence occurred, but when convergence did occur it affected the direction. When this feature was not present (that is, the plasticity rates of all input connections of a column were equal), the match between the *in vivo* and simulated convergence directions was degraded (for a more detailed description of both of these features, see **Supplementary Results**).

Convergence driven by competition for activity precedence

To clarify the fundamental difference in the reorganization generated by CDP and STDP, we ran simulations of the same model but with a lesion projection zone that was circular rather than asymmetric (as in the simulations that produced **Figs. 3** and **4**). When the gain increase inside the circular lesion projection zone was low ($1 < \beta < 1.1$), both CDP and STDP produced divergent receptive field shifts (**Fig. 5a**,**b**). This gain range was also associated with a specific form of activity dynamic, where activity that was propagated horizontally through the zone degraded with distance traveled. Before any reorganization, this dynamic generated a decreasing gradient of mean activity and an increasing gradient of response latency in the lesion projection zone (from its periphery to its center). When the neuronal gain increase was high ($\beta > 1.1$), the average activity among columns inside the lesion projection zone became higher than that of columns outside the zone. The combination of this activity distribution with CDP caused columns in the lesion projection zone to increase the efficacy of the horizontal input connections that they received from each other (**Fig. 5c**). Concomitantly, the efficacy of the input connections received from columns outside the zone decreased, but the receptive fields of columns inside the zone maintained their divergent shifts. Notably, however, the combination of high gain and STDP produced a strong unidirectional bias in the horizontal connectivity of the lesion projection zone columns and a corresponding convergence of their receptive fields (**Fig. 5d**), as it did with the asymmetrically shaped lesion projection zones (**Figs. 3b** and **4b**). Repeated runs of this simulation with feedforward input sequences of different random order showed that, as long as the lesion projection zone shape was circular, the direction in which the receptive field convergence develops was random. We also performed simulations with elliptical lesion projection zone shapes and observed that the resulting directions of receptive field convergence were biased toward the columns that were the most 'exposed' to horizontal input from outside the zone, namely, those columns located inside the two tips of the ellipse. For reasons explained below, the direction bias toward these exposed columns seems to arise from the high probability that, when activity flows into the lesion projection zone, it will flow through these exposed columns.

We sought to understand better how, in our model, STDP generates receptive field convergence. Consider again the example of didactic reorganization between two reciprocally connected neurons[18]: when the spike of neuron A precedes that of neuron B, the resulting changes in connection efficacies will make the response properties of neuron B more similar to those of neuron A; however, they will also contribute to making the spike order A to B more likely to occur in the future than the spike order B to A. Thus, neuron A, by undergoing spike precedence, is 'rewarded' by didactic reorganization

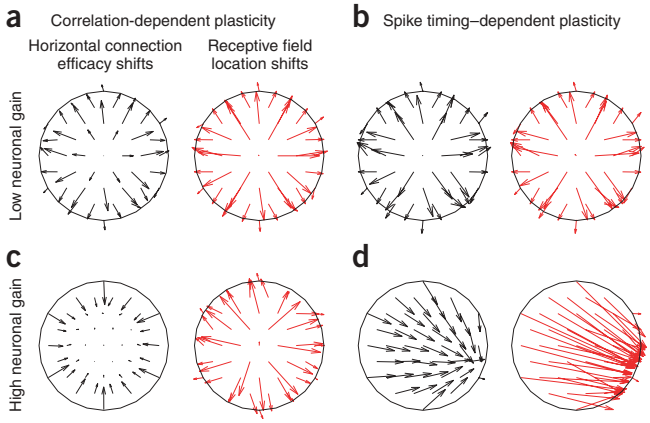

Figure 5 Simulated reorganization of receptive fields in a symmetric lesion projection zone, dependent on the strength of neuronal gain and use of CDP or STDP. (**a**) CDP combined with a small increase in neuronal gain ($\beta = 1.01$). (**b**) STDP combined with a small increase in neuronal gain ($\beta = 1.01$). (**c**) CDP combined with a large increase in neuronal gain ($\beta = 1.45$). (**d**) STDP combined with a large increase in neuronal gain ($\beta = 1.45$). All data are plotted in cortical space and the circular lesion projection zone used in these simulations is shown twice in each panel: on the left, each black arrow illustrates the change in the efficacy of the horizontal input connections to a single column (as in **Fig. 3**); on the right, each red arrow illustrates the change in position of the receptive field of a single column (as in **Fig. 3**).

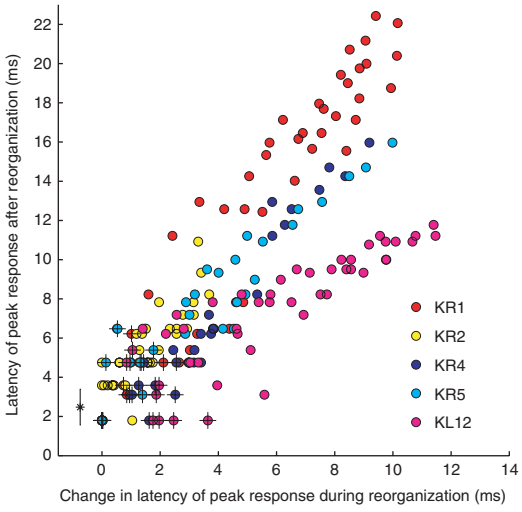

Figure 6 Latency of peak responses among the lesion projection zone columns of the model during and after STDP-based reorganization. The peak response latency (see Results) of each column in the lesion projection zone was calculated at regular intervals during the simulations that produced the receptive field convergence shown in **Figure 3b**. The *x* axis shows the mean difference between the peak response latency of each column immediately after lesioning (but before reorganization) and all its latencies measured during reorganization. The *y* axis shows the peak response latency of each column after reorganization. To illustrate further the general increase in peak response latency that accompanied reorganization, the pre-reorganization peak response latencies from all five simulations were pooled and the mean (asterisk) and standard deviation (error bars) of this combined distribution are indicated (relative to the *y* axis). The *x* and *y* axis values of each data point were added together and, for each lesion projection zone shape, the eight data points that had the lowest combined values are marked with a '+'. The columns to which these data points belong are also marked in **Figure 3b** with a '+'.

with connectivity changes that increase its future probability of spike precedence. The effect of this feedback loop is to make neurons A and B 'compete', through connectivity changes, to achieve the highest probability of spike precedence.

Consider now a chain of reciprocally connected neurons that is capable of propagating activity across its length: the didactic reorganization event described above for neurons A and B would be replicated by each consecutive neuron pair as activity propagates along the chain. Notably, this replication would allow didactic reorganization, and the ensuing competition for spike precedence, to occur between all neurons in the network, even those that are not monosynaptically connected. The range of didactic reorganization would be restricted only if there is a limit on the distance over which individual waves of activity can propagate. The competition for spike precedence would be expected to continue until connective changes establish a dominant hierarchy of spike timing within the network, in which neurons at the top consistently fire first, and those at the bottom fire last. An additional effect of these connective changes would be that the receptive field locations of all of the neurons involved in the competition would come to resemble those of neurons at the top of this hierarchy, thereby producing receptive field convergence.

Consistent with the hypothesis described above, we observed that the receptive field convergence produced by the model is clearly associated with the establishment of a hierarchy of activity timing inside the lesion projection zone. At regular intervals during the simulations that produced the results shown in **Figures 3b** and **4b**, the latency (relative to the time of stimulus onset) of the maximal activation (or 'peak response') of each column was measured. Short latency of the peak response of a column indicates that the probability of spike precedence among neurons in this column (relative to neurons in other columns) is high. Comparison of **Figures 6** and **3b** shows that the direction of receptive field convergence in each case was toward the lesion projection zone columns that maintained the shortest peak response latencies during reorganization (see also **Supplementary Videos**). In our model, propagation range is dependent on neuronal gain; thus, our hypothesis predicts that relatively low post-lesion increases in gain should restrict the range of didactic reorganization and the development of an activity-timing hierarchy. Consistent with this prediction, the relatively small gain increase ($\beta = 1.25$) used in the KR2 STDP simulation produced a relatively weak hierarchy of peak response latencies (**Fig. 6**) and multiple points of receptive field convergence (**Fig. 3b**).

DISCUSSION

We have compared *in vivo* and simulated receptive field location changes that are triggered among V1 neurons by a monocular retinal lesion made during postnatal development. A post-lesion increase in neuronal gain among the simulated lesion projection zone neurons led to an immediate expansion and radial shift of their receptive fields, such that they became responsive to stimuli presented outside the retinal lesion. It has been observed[30,32,39] that this expansion and shifting of receptive fields, in addition to the transition from inactivity to responsiveness, occur within hours of lesion creation *in vivo*. Long-term experiments have shown that these receptive field changes are associated with abnormally high evoked and 'spontaneous' (background) firing rates among neurons inside the lesion projection zone[24], which further supports the hypothesis that these changes come about through an increase in gain. A possible mechanism by which this gain increase could occur is synaptic scaling[40], because this phenomenon can be triggered in visual cortex through a decrease in feedforward input[41]. In addition, synaptic scaling also implements gain change by modifying the balance of excitation and inhibition within a network[42], which is consistent with the change in the balance of excitatory and inhibitory neurotransmitters that occurs in the lesion projection zone of V1 *in vivo*[43].

Much empirical evidence indicates that the initially expanded receptive fields of neurons in the lesion projection zone contract onto the retina surrounding the lesion owing to a long-term reorganization of the horizontal input connections intrinsic to V1 (refs. 33–35,44). Our simulation results support this hypothesis because Hebbian plasticity (either CDP or STDP) at the horizontal connections of the model produced receptive field contraction, even when the increased neuronal gain levels that caused the initial (post-lesion) receptive field expansion were maintained. When CDP was used, however, the directions of the receptive field shifts after reorganization did not resemble the directions that we observed in our *in vivo* experiments. When STDP was used, by contrast, the directions of the *in vivo* shifts and their convergent character were reproduced far more accurately. These simulations showed that an essential catalyst for the generation of receptive field convergence through STDP was an increase in gain sufficient to extend significantly the range of activity propagation. Such gain levels also produced higher rates of firing inside the lesion projection zone of the model than outside, which (as mentioned above) is a phenomenon that has been reported after retinal lesions *in vivo*[24].

Our modeling work indicates that receptive field convergence emerges from a competition between neurons in the lesion projection

zone for control over the timing of each other's activity. Underlying this competition is STDP-based didactic reorganization, which consists of incremental plasticity events in which response properties, including spike-timing, are unilaterally transferred between neurons[18]. In our model, the spatial range of didactic reorganization is dependent on the range of activity propagation, and is therefore affected by changes in neuronal gain. At low gain, didactic reorganization occurs only between nearby columns, producing receptive field shifts that are very similar to those that occur when CDP is used. At high gain, however, this reorganization can occur among all columns inside the lesion projection zone, causing all columns to compete with each other, which in turn generates receptive field convergence. This competition can be biased to favor specific neurons by increasing their probability of spiking early during the spread of activity in the lesion projection zone, thereby explaining why the shape of the zone influences the direction in which receptive field convergence develops.

Intriguingly, it has been observed that there are juvenile critical periods in V1 during which input deprivation can induce stronger increases in neuronal gain than those induced in adulthood[41]. If our reorganization hypothesis is correct, the *in vivo* receptive field shifts that we have observed are an extreme instance of didactic reorganization, triggered by an abnormally large increase in neuronal gain. The apparent capacity of STDP to produce ordered and effective connectivity patterns[18] suggests, however, that more moderate and localized gain increases could extend the spatial scale of didactic reorganization subtly enough for it to play a constructive role in the developmental organization of connectivity. Considering also that the critical periods for neuronal gain modulation referred to above are specifically regulated according to cortical layer[40], and that these layers seem to guide each other in a hierarchical, activity-dependent manner[45], it would be interesting to explore the possibility that didactic reorganization is dynamically regulated as a functional component of activity-dependent development.

Critical periods for neuronal gain modification are also relevant to our study because they occur at a stage of development that corresponds to the age at which the cats involved received their retinal lesions[41]. It is difficult to compare the results of retinal lesion experiments performed in different laboratories owing to differences in lesion size and location, and differences in the mono-/binocularity of the lesion. Nonetheless, it is worth noting that most previous studies, which did not describe observing convergence among receptive field shifts after long-term reorganization, made their retinal lesions in adult animals[26,32,33]. We observed in our model that when neuronal gain levels are increased only moderately (thereby limiting the spatial range of didactic reorganization), STDP, like CDP, produces a divergent pattern of receptive field shifts. It is therefore possible that STDP occurs at the V1 horizontal connections of both adolescent and adult animals, but that receptive field convergence is more likely to be observed in the former owing to their enhanced capacity for increases in neuronal gain. Assuming that the plasticity at horizontal cortical connections is dependent on spike timing, a weaker capacity for gain change in adult animals might also explain the apparent consistency between the results of CDP models and previous examples of *in vivo* cortical reorganization[12,15,16]. One other group has made monocular lesions in cats of a similar age to that of the cats involved in this study[27]. Because their study focused on a different aspect of post-lesion reorganization, however, the vergence of the receptive field shifts that they observed is difficult to assess.

There is conflicting evidence concerning whether long-term receptive field organization in cortex is spike timing– or correlation-dependent[13–18,20,21]. To our knowledge, our study is the first to identify an aspect of long-term reorganization in V1 that is not only highly consistent with the former hypothesis, but also highly inconsistent with the latter. Short-term studies have shown that temporally specific stimulation of neurons *in vivo* produces subtle receptive field changes that are consistent with STDP[19,22]. Our results indicate that, during a prolonged input perturbation, such acute spike timing–dependent changes accrue to produce far more extreme and consolidated receptive field modifications, like those that we have observed *in vivo*. Consistent with previous studies, our results also provide evidence that a partial loss of input to the cortical circuit triggers a process of reorganization involving large increases in neuronal gain, possibly through the mechanism of synaptic scaling. In our model, this increase in gain alters cortical activity propagation, which in turn extends the spatial range of STDP-based didactic reorganization, and the ensuing competition for the control of activity timing generates receptive field convergence.

METHODS

Cortical recordings. All experimental and animal care procedures followed the guidelines of the Australian Code of Practice for the Care and Use of Animals for Scientific Purposes and were approved by the Animal Care Ethics Committees at the University of Sydney and the Australian National University. The number of weeks between the creation of the retinal lesion (made under anesthesia using an argon-green laser) and recording in each case was as follows: KR1, 29; KR2, 30; KR4, 43; KR5, 47; KL12, 63. All receptive field data were gathered via extracellular single-cell recordings in V1 (striate cortex, cytoarchitectonic area 17) in deeply anesthetized cats. Receptive field location and orientation preference were determined using hand-held stimuli and were verified whenever possible through automated methods. In each experiment, we determined the retinal lesion shape (**Fig. 2**) by tracing on a tangent screen the image back-projected by the lesioned eye when light was shone through the dilated pupil. The density contours shown in **Figure 2** are from counts of α ganglion cells made on retinal whole mounts after the cortical recordings were complete. Details of the creation of retinal lesions, cortical recordings and histology in these experiments are available in the **Supplementary Methods** (see also ref. 28). Our control data (**Fig. 2**) comes from a separate set of experiments performed in the same laboratory using the same equipment and mapping techniques, and conducted by predominantly the same researchers.

Modeling. The aim of this model was to predict the retinal lesion–induced changes in receptive field position caused by reorganization of the long-range horizontal connections in the lesion projection zone of cat V1. The model used either STDP or CDP to modify the efficacy of horizontal connections between neighboring neuron populations (columns). A more detailed description of the model is given in the **Supplementary Methods**.

Connective architecture. The model network consisted of 18 × 18 cortical columns arranged in a hexagonal lattice with a spatial scale of 11 × 9.25 mm (unequal scale owing to hexagonal asymmetry). Each column represented a population of neurons and had both feedforward input connections and reciprocal horizontal connections with nearby columns. The model assumed that excitatory neurons in V1 receive most of their inhibition from local interneurons, and that excitatory and inhibitory neurons in the same column have similar horizontal input connections[46,47]. The initial strengths of the horizontal input connections of each column were given by:

$$w_{ij}^{\text{horiz}} = \begin{cases} \exp(-x_{ij}^2/1.56\,\text{mm}) & \text{if} \quad |x_{ij}| \le 2.5\,\text{mm} \\ 0 & \text{if} \quad |x_{ij}| > 2.5\,\text{mm} \end{cases} \qquad (1)$$

where w_{ij}^{horiz} is the efficacy of the input connection received by the postsynaptic column i from the presynaptic column j, and x_{ij} is the distance between columns i and j (in millimeters). Equation (1) is derived from previously made intracellular recordings[48] (fitted to Fig. 2c in ref. 48).

Activity. The proportion (v) of excitatory neurons in column i that underwent an action potential as a consequence of stimulus presentation was given by:

$$v_i = u_i \cdot w_i^{\mathrm{ff}} \cdot \beta + \sum_{j=1}^{n} v_j \cdot w_{ij}^{\mathrm{horiz}} \cdot (\beta - 1) \cdot \theta_{ij}(t_i^{\mathrm{pri}}, t_{ij}^{\mathrm{sec}}) \quad (2)$$

where u_i is the feedforward input received by column i, w_i^{ff} is the afferent feedforward connection weight, β is the neuronal gain, and θ_{ij} is a variable that modulates the efficacy of input of column j to column i depending on the relative timing of their initial responses during stimulus presentation (see below). Hard limits were imposed on v_i such that its value could not fall below 0 or rise above 1. The inclusion of $\beta - 1$ for modulating the strength of horizontal input takes into account the observation that, at normal gain levels ($\beta = 1$), input through long-range horizontal connections remains largely subthreshold because it evokes a roughly balanced mixture of excitation and inhibition[49]. Increasing the value of β then emulates the empirical phenomenon of synaptic scaling[40], where this balance is shifted in favor of excitation by nonselectively potentiating the excitatory afferents to excitatory neurons and nonselectively depressing the excitatory afferents to inhibitory neurons[42].

The function θ_{ij} in equation (2) reduces the responsiveness of a column to input immediately after the initial activation of that column. It is given by:

$$\theta_{ij} = 1 + (t_i^{\mathrm{pri}} - t_{ij}^{\mathrm{sec}})/\tau^{\theta} \quad (3)$$

where t_i^{pri} is the arrival time (in milliseconds) of the first input of column i (either feedforward or horizontal) during stimulus presentation, t_{ij}^{sec} is the arrival time of horizontal input from column j, and τ^{θ} (1 ms) is the time window during which input can be integrated into the activation of column i before complete suppression. Values of θ_{ij} below 0 were set to 0. The first input to arrive at a model column was always defined as suprathreshold. Because the values of t_i^{pri} and t_{ij}^{sec} were based on cortical distance and an empirical measure of propagation velocity[49], θ_{ij} remained constant during reorganization. The effects of θ_{ij} on network activity are consistent with the wave-like cortical activity dynamics that have been observed *in vitro*[37] and *in vivo*[38]. Such dynamics are probably caused by the locally mediated inhibitory input that accompanies excitatory input from horizontal connections[49], and/or fast-acting depression at the afferent excitatory synapses of excitatory neurons combined with fast-acting facilitation at the afferent excitatory synapses of inhibitory neurons[7]. In theory, spike probability in each column is suppressed only transiently, thereby allowing neurons in the column to produce spike trains. Experimental work has shown, however, that synaptic change among horizontal connections in layers 2/3 of mammalian V1 depends primarily on the timing of the first pre- and postsynaptic spikes within the spike trains of connected neurons[10]. Because we are interested in activity only in so far as it influences plasticity, we use equation (2) as a description of the initial activation that occurs in each column as a consequence of feedforward stimulus presentation, and not as a description of ongoing stimulus-evoked activation. Equation (2) was solved by numeric integration (Euler method) of its differential form.

Plasticity. Each input presentation consisted of activating the feedforward input to a single randomly selected column outside the lesion projection zone ('nonlesion projection zone') under the condition that all nonlesion projection zone columns had to receive input exactly once before each weight update step. We simulated the effect of a retinal lesion by preventing columns within the lesion projection zone from receiving feedforward input. After each stimulus presentation, change in the efficacy of the horizontal input connection from column j to column i, w_{ij}^{horiz}, was calculated by using either STDP or CDP, and the accumulated changes arising from multiple stimulus presentations were added to w_{ij}^{horiz} in a subsequent weight update step. The STDP rule took the form:

$$\Delta w_{ij}^{\mathrm{horiz}} = v_i \cdot v_j \cdot F(\Delta t_{ij}) \cdot \alpha_{ij} \quad (4)$$

where F is the STDP transfer function (see below), and α_{ij} is the specific learning rate of the input connection from the presynaptic (j) to the postsynaptic (i) column (see below). The term $v_i\, v_j$ makes the weight change dependent on the proportion of neurons in each population that are active as a consequence of stimulus presentation. The variable Δt_{ij} is given by $\Delta t_{ij} = t_i^{\mathrm{pri}} + t^{\mathrm{SI}} - t_{ij}^{\mathrm{sec}}$, where t^{SI} (0.4 ms) is the time required for spike initiation. F was calculated as:

$$F(\Delta t_{ij}) = \begin{cases} A_+ \exp(-\Delta t_{ij}/\tau_+) & \text{if} \quad \Delta t_{ij} \geq 0 \\ -A_- \exp(\Delta t_{ij}/\tau_-) & \text{if} \quad \Delta t_{ij} < 0 \end{cases} \quad (5)$$

where the upper and lower expressions refer to long-term potentiation and long-term depression, respectively. The parameter values are $A_+ = 1.01$, $A_- = 0.52$, $\tau_+ = 14.8$ ms, and $\tau_- = 33.8$ ms (from recordings in rat visual cortex[10]).

The learning rate value α_{ij} is proportional to the distance between the presynptic (j) and postsynaptic (i) columns and is given by the right hand side of equation (1), multiplied by a scaling factor. The value of this scaling factor was not critical for the reorganization results and was adjusted to ensure that the CDP and STDP simulations had comparable rates of plasticity. The values of α_{ij} for all of the horizontal input connections received by nonlesion projection zone columns were zero. A more detailed rationale for this rate-based approximation of STDP can be found in the **Supplementary Methods**.

CDP was implemented as a standard 'Hebbian' learning rule:

$$\Delta w_{ij}^{\mathrm{horiz}} = v_i \cdot v_j \cdot \alpha_{ij} \quad (6)$$

Making all values of α_{ij} equal had no significant effect on the results produced by the CDP rule, but for the sake of comparison the results shown in **Figure 3a** were produced by using the values of α_{ij} that were used in the STDP simulation. For both STDP and CDP, the total synaptic weight of the horizontal inputs to each column was constrained through multiplicative normalization, and any connection weight below 0.02 was set to 0, which effectively prevented the connection from undergoing any further change[50].

When STDP was used, training was stopped when the network had reached its best achievable match with the corresponding *in vivo* results, as assessed by the mean distance between the simulated and *in vivo* receptive field centers in addition to the difference between the simulated and *in vivo* vergence values. In each case, the average rate of weight change among the lesion projection zone columns (normalized relative to the peak value) was <0.15 when training was stopped. When the CDP rule was used, the training duration had little impact on the final match with the *in vivo* data; thus, training was halted when all weight change had effectively ceased. The procedure for mapping receptive fields in the model is given in the **Supplementary Methods**.

Note: Supplementary information is available on the Nature Neuroscience website.

ACKNOWLEDGMENTS

We thank W. Burke for participating in the experimental work; J.Y. Huang for participating in the control experiments; T. Hoch for modeling advice; and K. Wimmer, E. Mukamel, L. Schwabe, T. Hoch and R. Martin for manuscript comments. Support was contributed by the Australian Research Council, the Bernstein Center for Computational Neuroscience Berlin, the German Federal Ministry of Education and Research (BMBF, grant 10025304), and the German Academic Exchange Service (DAAD).

AUTHOR CONTRIBUTIONS

J.M.Y., W.J.W., C.W. and B.D. conducted the experimental work and analyzed the collected data. M.B.C. made the retinal lesions. B.D. and M.B.C. designed the experiments. K.O. supervised the modeling project, which included providing guidance on the choice of model type and advice on the model's abstractions. J.M.Y. conceived the modeling project and conducted the modeling work, which included developing the model's novel abstractions. The manuscript was drafted primarily by J.M.Y., but all the authors were actively involved in its refinement.

COMPETING INTERESTS STATEMENT

The authors declare no competing financial interests.

Published online at http://www.nature.com/natureneuroscience
Reprints and permissions information is available online at http://npg.nature.com/reprintsandpermissions

1. Hubel, D.H. & Wiesel, T.N. Binocular interaction in striate cortex of kittens reared with artificial squint. *J. Neurophysiol.* **28**, 1041–1059 (1965).
2. Katz, L.C. & Shatz, C.J. Synaptic activity and the construction of cortical circuits. *Science* **274**, 1133–1138 (1996).
3. Hebb, D.O. *The Organization of Behaviour* (John Wiley & Sons, New York, 1949).
4. Stent, G.S. A physiological mechanism for Hebb's postulate of learning. *Proc. Natl. Acad. Sci. USA* **70**, 997–1001 (1973).

5. Malenka, R.C. & Nicoll, R.A. NMDA receptor–dependent synaptic plasticity: multiple forms and mechanisms. *Trends Neurosci.* **16**, 521–527 (1993).
6. Levy, W.B. & Steward, O. Temporal contiguity requirements for long-term associative potentiation/depression in the hippocampus. *Neuroscience* **8**, 791–797 (1983).
7. Markram, H., Lubke, J., Frotscher, M. & Sakmann, B. Regulation of synaptic efficacy by coincidence of postsynaptic APs and EPSPs. *Science* **275**, 213–215 (1997).
8. Song, S., Miller, K.D. & Abbott, L.F. Competitive Hebbian learning through spike-timing–dependent synaptic plasticity. *Nat. Neurosci.* **3**, 919–926 (2000).
9. Sjöström, P.J., Turrigiano, G.G. & Nelson, S.B. Rate, timing, and cooperativity jointly determine cortical synaptic plasticity. *Neuron* **32**, 1149–1164 (2001).
10. Froemke, R.C. & Dan, Y. Spike-timing–dependent synaptic modification induced by natural spike trains. *Nature* **416**, 433–438 (2002).
11. Dan, Y. & Poo, M.-M. Spike timing–dependent plasticity of neural pircuits. *Neuron* **44**, 23–30 (2004).
12. Pearson, J.C., Finkel, L.H. & Edelman, G.M. Plasticity in the organization of adult cerebral cortical maps: a computer simulation based on neuronal group selection. *J. Neurosci.* **7**, 4209–4223 (1987).
13. Obermayer, K., Ritter, H. & Schulten, K. A principle for the formation of the spatial structure of cortical feature maps. *Proc. Natl. Acad. Sci. USA* **87**, 8345–8349 (1990).
14. Hirsch, J.A. & Gilbert, C.D. Long-term changes in synaptic strength along specific intrinsic pathways in the cat visual cortex. *J. Physiol. (Lond.)* **461**, 247–262 (1993).
15. Xing, J. & Gerstein, G.L. Networks with lateral connectivity. 3. Plasticity and reorganization of somatosensory cortex. *J. Neurophysiol.* **75**, 217–232 (1996).
16. Miikkulainen, R., Bednar, J.A., Choe, Y. & Sirosh, J. Self-organization, plasticity and low-level visual phenomena in a laterally connected map model of the primary visual cortex. in *Psychology of Learning and Motivation: Perceptual Learning* (eds. Goldstone, R.L., Schyns, P.G. & Medin, D.L.) 257–308 (Academic Press, San Diego, 1997).
17. Feldman, D.E. Timing-based LTP and LTD at vertical inputs to layer II/III pyramidal cells in rat barrel cortex. *Neuron* **27**, 45–56 (2000).
18. Song, S. & Abbott, L.F. Cortical development and remapping through spike timing–dependent plasticity. *Neuron* **32**, 339–350 (2001).
19. Fu, Y.X. *et al.* Temporal specificity in the cortical plasticity of visual space representation. *Science* **296**, 1999–2003 (2002).
20. Eyding, D., Schweigart, G. & Eysel, U.T. Spatio-temporal plasticity of cortical receptive fields in response to repetitive visual stimulation in the adult cat. *Neuroscience* **112**, 195–215 (2002).
21. Celikel, T., Szostak, V.A. & Feldman, D.E. Modulation of spike timing by sensory deprivation during induction of cortical map plasticity. *Nat. Neurosci.* **7**, 534–541 (2004).
22. Meliza, C.D. & Dan, Y. Receptive-field modification in rat visual cortex induced by paired visual stimulation and single-cell spiking. *Neuron* **49**, 183–189 (2006).
23. Pettigrew, J.D. The effect of visual experience on the development of stimulus specificity by kitten cortical neurones. *J. Physiol. (Lond.)* **237**, 49–74 (1974).
24. Giannikopoulos, D.V. & Eysel, U.T. Dynamics and specificity of cortical map reorganization after retinal lesions. *Proc. Natl. Acad. Sci. USA* **103**, 10805–10810 (2006).
25. Olson, C.R. & Freeman, R.D. Profile of the sensitive period for monocular deprivation in kittens. *Exp. Brain Res.* **39**, 17–21 (1980).
26. Kaas, J.H. *et al.* Reorganization of retinotopic cortical maps in adult mammals after lesions of the retina. *Science* **248**, 229–231 (1990).
27. Chino, Y. *et al.* Recovery of binocular responses by cortical neurons after early monocular lesions. *Nat. Neurosci.* **4**, 689–690 (2001).
28. Waleszczyk, W.J. *et al.* Laminar differences in plasticity in cat area 17 following retinal lesions in adolescence or adulthood. *Eur. J. Neurosci.* **17**, 2351–2368 (2003).
29. Fitzgibbon, T., Funke, K. & Eysel, U.T. Anatomical correlations between soma size, axon diameter and intraretinal length for the α ganglion cells of the cat retina. *Vis. Neurosci.* **6**, 159–174 (1991).
30. Calford, M.B., Schmid, L.M. & Rosa, M.G.P. Monocular focal retinal lesions induce short-term topographic plasticity in adult cat visual cortex. *Proc. Biol. Soc.* **266**, 499–507 (1999).
31. Calford, M.B. *et al.* Plasticity in adult cat visual cortex (area 17) following circumscribed monocular lesions of all retinal layers. *J. Physiol. (Lond.)* **524**, 587–602 (2000).
32. Gilbert, C.D. & Wiesel, T.N. Receptive field dynamics in adult primary visual cortex. *Nature* **356**, 150–152 (1992).
33. Darian-Smith, C. & Gilbert, C.D. Topographic reorganization in the striate cortex of the adult cat and monkey is cortically mediated. *J. Neurosci.* **15**, 1631–1647 (1995).
34. Calford, M.B., Wright, L.L., Metha, A.B. & Taglianetti, V. Topographic plasticity in primary visual cortex is mediated by local corticocortical connections. *J. Neurosci.* **23**, 6434–6442 (2003).
35. Young, J.M., Waleszczyk, W.J., Burke, W., Calford, M.B. & Dreher, B. Topographic reorganization in area 18 of adult cats following circumscribed monocular retinal lesions in adolescence. *J. Physiol. (Lond.)* **541**, 601–612 (2002).
36. Tusa, R.J., Palmer, L.A. & Rosenquist, A.C. The retinotopic organization of area 17 (striate cortex) in the cat. *J. Comp. Neurol.* **177**, 213–235 (1978).
37. Tanifuji, M., Sugiyama, T. & Murase, K. Horizontal propagation of excitation in rat visual cortical slices revealed by optical imaging. *Science* **266**, 1057–1059 (1994).
38. Jancke, D., Chavane, F., Naaman, S. & Grinvald, A. Imaging cortical correlates of illusion in early visual cortex. *Nature* **428**, 423–426 (2004).
39. Chino, Y.M., Kaas, J.H., Smith, E.L., III, Langston, A.L. & Cheng, H. Rapid reorganization of cortical maps in adult cats following restricted deafferentation in retina. *Vision Res.* **32**, 789–796 (1992).
40. Turrigiano, G.G., Leslie, K.R., Desai, N.S., Rutherford, L.C. & Nelson, S.B. Activity-dependent scaling of quantal amplitude in neocortical neurons. *Nature* **391**, 892–896 (1998).
41. Desai, N.S., Cudmore, R.H., Nelson, S.B. & Turrigiano, G.G. Critical periods for experience-dependent synaptic scaling in visual cortex. *Nat. Neurosci.* **5**, 783–789 (2002).
42. Rutherford, L.C., Nelson, S.B. & Turrigiano, G.G. BDNF has opposite effects on the quantal amplitude of pyramidal neuron and interneuron excitatory synapses. *Neuron* **21**, 521–530 (1998).
43. Arckens, L. *et al.* Cooperative changes in GABA, glutamate and activity levels: the missing link in cortical plasticity. *Eur. J. Neurosci.* **12**, 4222–4232 (2000).
44. Darian-Smith, C. & Gilbert, C.D. Axonal sprouting accompanies functional reorganization in adult cat striate cortex. *Nature* **368**, 737–740 (1994).
45. Trachtenberg, J.T. & Stryker, M.P. Rapid anatomical plasticity of horizontal connections in the developing visual cortex. *J. Neurosci.* **21**, 3476–3482 (2001).
46. Anderson, J.S., Carandini, M. & Ferster, D. Orientation tuning of input conductance, excitation and inhibition in cat primary visual cortex. *J. Neurophysiol.* **84**, 909–926 (2000).
47. Yoshimura, Y. & Callaway, E.M. Fine-scale specificity of cortical networks depends on inhibitory cell type and connectivity. *Nat. Neurosci.* **8**, 1552–1559 (2005).
48. Bringuier, V., Chavane, F., Glaeser, L. & Frégnac, Y. Horizontal propagation of visual activity in the synaptic integration field of area 17 neurons. *Science* **283**, 695–699 (1999).
49. Hirsch, J.A. & Gilbert, C.D. Synaptic physiology of horizontal connections in the cat's visual cortex. *J. Neurosci.* **11**, 1800–1809 (1991).
50. Colman, H., Nabekura, J. & Lichtman, J.W. Alterations in synaptic strength preceding axon withdrawal. *Science* **275**, 356–361 (1997).